

Cancer chemoprevention by the antioxidant tempol in *Atm*-deficient mice

Ralf Schubert^{1,2,3,†}, Laura Erker^{1,2,3,†}, Carolee Barlow^{4,‡}, Hiroyuki Yakushiji^{1,2,3,¶},
Denise Larson⁴, Angelo Russo⁵, James B. Mitchell⁵ and Anthony Wynshaw-Boris^{1,2,3,4,*}

¹Department of Pediatrics, ²Department of Medicine and ³The Comprehensive Cancer Center, UCSD School of Medicine, La Jolla, CA, USA, ⁴Genetic Disease Research Branch, NHGRI and ⁵Radiation Biology Branch, NCI, Bethesda, MD, USA

Received April 28, 2004; Revised and Accepted June 11, 2004

Reactive oxygen species (ROS) are important endogenous etiological agents for DNA damage, and ROS perform critical signaling functions in apoptosis, stress responses and proliferation. The correlation between a lower incidence of cancer in people who consume a diet high in naturally occurring antioxidants and the observed increased ROS in cancerous tissues suggest that antioxidants may be used in cancer chemoprevention. We tested this hypothesis by determining whether the well-described nitroxide antioxidant, tempol (4-hydroxy-2,2,6,6-tetramethylpiperidine-*N*-oxyl), acts as a chemopreventative agent in *Atm* mutant mice, a model of the human cancer prone syndrome ataxia-telangiectasia. Tempol administered continuously via the diet after weaning resulted in an increased lifespan of these mice by prolonging the latency to thymic lymphomas. Tempol treatment reduced ROS, restored mitochondrial membrane potential, reduced tissue oxidative damage and oxidative stress, consistent with antioxidant effects. In addition, this nitroxide lowered weight gain of tumor prone mice without changes in food intake, metabolism or activity level and exhibited an anti-proliferative effect *in vitro*. Thus, tempol acts as a novel chemopreventative agent in this mouse model of a human cancer prone syndrome, associated with broad antioxidant effects.

INTRODUCTION

Reactive oxygen species (ROS) are produced in all mammalian cells from mitochondrial oxidative respiration or exposure to toxicants (1). Cellular defense mechanisms have evolved to protect cells from ROS, and these include repair systems, detoxifying enzymes such as superoxide dismutases (SODs), and small molecule scavengers such as glutathione (1). An imbalance between the mechanisms that generate and protect against ROS results in compensatory oxidative stress or even oxidative damage, including DNA damage (2). In addition to these deleterious effects, ROS appear to have necessary signaling functions in the modulation of apoptosis, stress and proliferative signaling pathways (3–8). These observations suggest that ROS may be an important target for cancer chemoprevention. Consistent with this notion, mouse knock-outs of *prdx1*, the gene encoding a ROS scavenger and antioxidant protein peroxiredoxin 1, display susceptibility to tumors (9).

Although a number of studies have examined the chemopreventative effect of antioxidants such as vitamins C and E, carotenoids and selenium (10), these studies have not provided consistent evidence in favor of such effects. To directly address the role of ROS in cancer and potential antioxidant chemoprevention, we studied the effects of chronic administration of a nitroxide antioxidant, tempol (4-hydroxy-2,2,6,6-tetramethylpiperidine-*N*-oxyl), on longevity and tumor formation in tumor prone *Atm*-deficient mice, a model of the human cancer prone syndrome ataxia-telangiectasia (AT). AT results from mutations in the ATM kinase, a member of a family that includes P-13 and DNA-PKcs kinase (11,12). ATM is essential for checkpoint and repair responses to double strand DNA damage (13,14). AT is a pleiotropic syndrome consisting of neuronal degeneration, oculocutaneous telangiectasias, growth retardation, infertility, sensitivity to ionizing radiation (IR) or agents that cause double stranded DNA breaks, immunodeficiencies and cancer predisposition,

*To whom correspondence should be addressed at: School of Medicine, University of California, San Diego, 9500 Gilman Drive, Mail Stop 0627, La Jolla, CA, 92093-0627, USA. Tel: +1 8588223400; Fax: +1 8588223409; Email: awynshawboris@ucsd.edu

†The authors wish it to be known that, in their opinion, the first two authors should be regarded as joint First Authors.

‡Present address: Merck Research Laboratories, San Diego, CA, USA.

¶Present address: Department of Surgery, Taku Hospital, Saga, Japan.

particularly lymphoreticular malignancies (15). Rotman and Shiloh (16) suggested that many of the features of AT are consistent with increased oxidative stress and/or damage, and several groups demonstrated that oxidative stress is increased in cell lines from human patients with AT (17,18) and in tissues from *Atm*^{-/-} mice (19–22).

Tempol was chosen for these experiments for several reasons. Tempol is one of a family of well-described stable nitroxides that detoxify oxygen metabolites by redox cycling via one-electron transfer reactions (23–27). It has SOD mimetic activity and confers catalase activity to heme proteins (28–31). It protects cells and animals from oxidative stress (32–35). Finally, long-term tempol treatment resulted in a reduction of tumor incidence in wild-type C3H mice (36). In support of a chemopreventative role of antioxidants, our studies demonstrate a significantly increased latency of tumors in the *Atm*-deficient model of this human cancer prone syndrome.

RESULTS

Tempol increases longevity of *Atm*^{-/-}

We tested the *Atm*-deficient mice (37) since these mice: (i) display increased oxidative stress and damage (19–22); (ii) demonstrate a highly penetrant lymphoma phenotype (37); (iii) have a short latency to develop tumors (37); and (iv) are an excellent model of the tumor phenotype of the human disease AT. Tempol was chronically administered in the diet of these animals to give a fairly constant dose throughout the treatment. Because tempol tastes bitter and unpleasant to mice, it was mixed with bacon-flavored mouse chow at 58 mM (10 mg/g of food) (36). A previous study with C3H mice demonstrated that the bitter taste of tempol reduced food intake (36). However, when bacon flavor was added to the tempol mouse chow, the food intake was similar to placebo chow. The *Atm*^{-/-} mice were placed into one of three treatment arms: (i) mice fed bacon-flavored mouse chow without drug (placebo); (ii) mice placed on tempol-laced chow at weaning (tempol at weaning); and (iii) mice born to females that were fed tempol chow prior to mating, then constantly during pregnancy, lactation and after weaning (tempol at fertilization). Both treatment regimens resulted in an average serum concentration of 90–100 μ M (data not shown). Treated and untreated wild-type mice died of natural causes and lived a normal murine lifespan of about 1.5 years (data not shown). When the *Atm*^{-/-} mice were treated with tempol, it was apparent that only mice treated at weaning had significantly increased longevity (62.4 versus 30.1 weeks, $P < 0.01$, Fig. 1A). However, the mean survival time for animals treated with tempol from fertilization (Fig. 1B) was unchanged (37.1 weeks, $P > 0.7$) from mice fed the placebo diet.

No effect of tempol treatment on tumor type in the *Atm*^{-/-} mice

Most animals from each group were autopsied. As previously shown for the *Atm*-deficient mice (37,38), the tempol-treated and placebo mice died from the same CD4⁺/CD8⁺ thymic lymphomas that contained 3–5 chromosomal translocations including both alleles of the TCR α δ locus (data not shown). An early event in the development of thymic lymphomas in

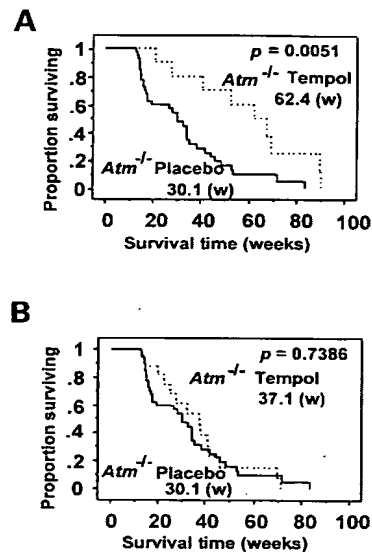


Figure 1. Survival curves of the *Atm*^{-/-} mice fed placebo or tempol containing mouse chow. Survival is shown in weeks (w). (A) Kaplan–Meier analysis for the *Atm*^{-/-} mice fed with a tempol diet at weaning (dashed line) or a placebo (solid line) diet. (B) The *Atm*^{-/-} mice fed with a tempol-containing diet from fertilization (before birth and after weaning, dashed line) or placebo diet (solid line).

the *Atm*^{-/-} mice are chromosome 14 translocations that occur in CD4⁺/CD8⁺ immature thymocytes at the point of V(D)J recombination in the TCR α δ locus (38). The frequency of these translocations arising in thymic development can be estimated in splenocytes. Since these translocations occur during embryonic development well before tempol treatment was initiated, we expected no differences between the placebo and tempol-treated mice, and no differences were found ($7.66 \pm 0.30\%$ for placebo group and $7.58 \pm 0.88\%$ for tempol group). These data are consistent with the interpretation that the chemopreventative effect of tempol resulted from the prolonged latency to tumors without affecting tumor type in the *Atm*-deficient mice. In addition, this data argue against the selective toxicity of tempol towards cells containing chromosome 14 translocations.

Tempol treatment results in decreased ROS, oxidative damage and oxidative stress *in vivo*

It was important to convincingly demonstrate and confirm that the known and well-documented antioxidant effects of the nitroxide tempol (23–27) were found in wild-type and *Atm*^{-/-} mice as well as primary cells treated with tempol. The effect of tempol treatment on intracellular ROS was determined by measuring the conversion of non-fluorescent 2'7'-dichlorodihydrofluorescein to the fluorescent 2'7'-dichlorodihydrofluorescein (DCF) quantitatively by flow cytometry (39–41). DCF fluorescence was significantly increased in thymocytes from the *Atm*^{-/-} mice relative to the wild-type (Fig. 2A and D). Tempol significantly reduced DCF intensity in thymocytes from both wild-type and *Atm*^{-/-} mice

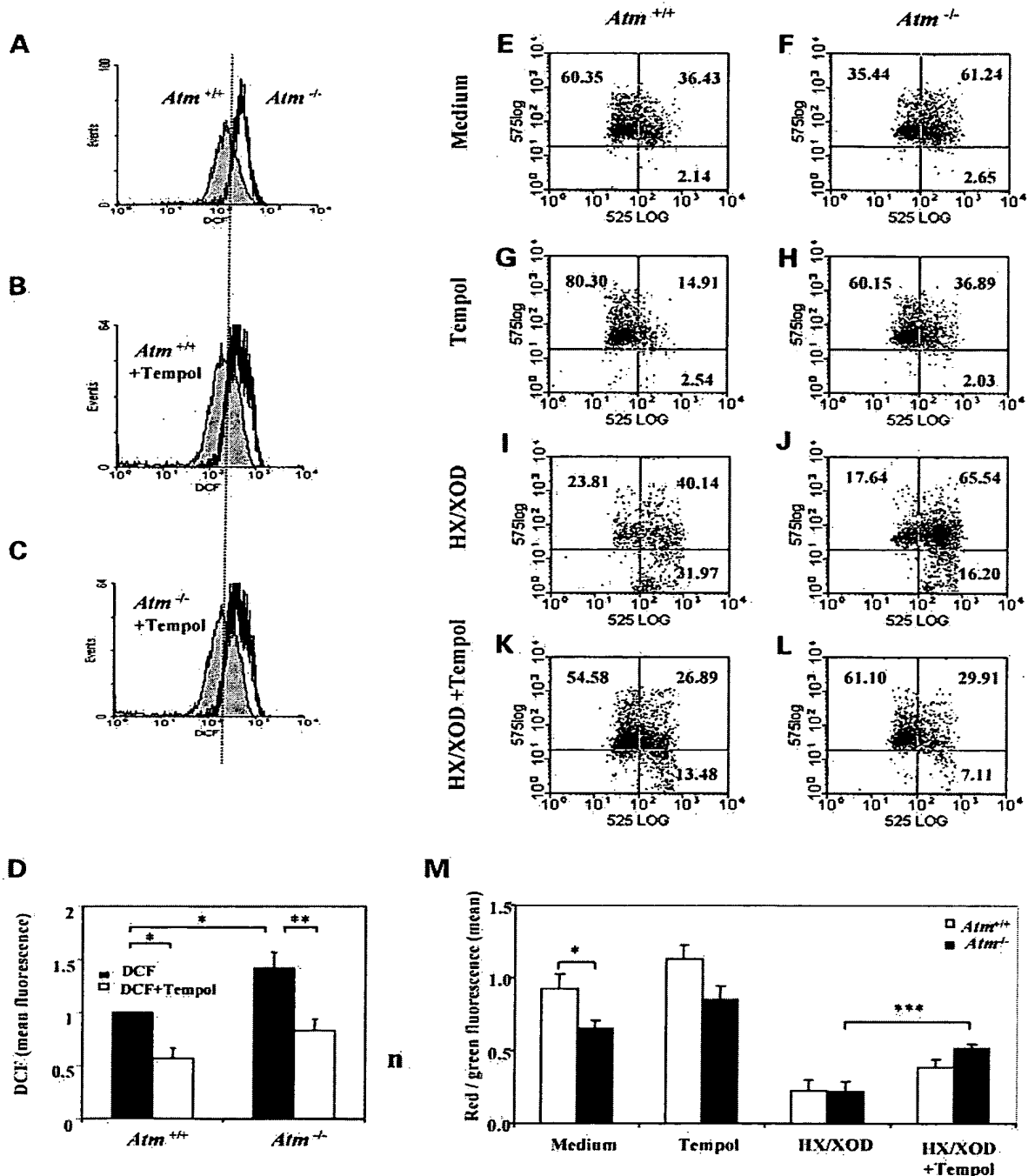


Figure 2. Influence of tempol on ROS and mitochondrial membrane potential ($\Delta\Psi_m$) after oxidative stress in primary thymocytes. The levels of ROS were measured via DCF fluorescence in primary thymocytes of the *Atm*^{+/+} and *Atm*^{-/-} mice treated with and without tempol. (A) FACS histogram of the *Atm*^{+/+} (clear) versus *Atm*^{-/-} (gray) ROS levels. (B) FACS histogram of the *Atm*^{+/+} placebo (clear) versus *Atm*^{+/+} mouse thymocytes treated with tempol (gray). (C) FACS histogram of the *Atm*^{-/-} control (gray) versus *Atm*^{-/-} mouse thymocytes treated with tempol (clear). (D) Quantitative analysis of ROS levels with (clear) and without (black) tempol measured as fold change from untreated *Atm*^{+/+}. Analysis of $\Delta\Psi_m$ on primary thymocytes from the *Atm*^{+/+} and *Atm*^{-/-} mice by JC-1 flow cytometry. (E, F) Representative dot plots of untreated cells, (G, H) tempol-treated cells (1 mM), (I, J) cells treated with HX 0.1 mM, XOD 10 mU/ml and (K, L) cells treated with HX/XOD and tempol, from the *Atm*^{+/+} (left panels) and *Atm*^{-/-} mice (right panels). (M) Graph represents quantitative analysis of the ratio of red (575 nm) and green fluorescence (525 nm) of four independent experiments for each genotype and treatment. Data are shown as mean \pm SEM (**P* < 0.05; ***P* < 0.01; ****P* < 0.005).

(Fig. 2B–D). These data are consistent with the interpretation that there is an increase in ROS in cells from *Atm*^{-/-} mice, and that tempol treatment reduces ROS.

If the difference in DCF fluorescence represented differences in ROS, then we expected that mitochondrial membrane potential ($\Delta\psi_m$) should be altered as well. Mitochondria are one of the major sources of ROS via oxidative phosphorylation, and the first target of ROS-induced damage (42). Changes in the $\Delta\psi_m$ caused by ROS are a suitable indicator of mitochondrial integrity as well as for apoptotic activity. We used the lipophilic cation 5,5',6,6'-tetrachloro-1,1',3,3'-tetraethylbenzimidazol-carbocyanine iodide (JC-1) to examine the influence of tempol on the $\Delta\psi_m$ of the wild-type and *Atm*^{-/-} thymocytes. JC-1 enters selectively into mitochondria and forms reversible aggregates that display both red (575 nm) and green (525 nm) fluorescence. Loss of $\Delta\psi_m$ results in an increase in green as well as a decrease in red JC-1 fluorescence (43), detected by a two color flow-cytometry assay. Thus, the ratio of red/green fluorescence provides a measure of mitochondrial membrane integrity. Treatment of thymocytes with 100 nM valinomycin to induce apoptosis and lower $\Delta\psi_m$ resulted in a shift in cells to the lower right quadrant (increase in green and decrease in red JC-1 fluorescence) and reduced the ratio of red/green fluorescence (data not shown).

In thymocytes from the wild-type mice, there were two fluorescent populations, on the basis of the amount of green fluorescence, with a 2:1 ratio of cells in the upper left (representing the highest $\Delta\psi_m$) versus upper right quadrants (Fig. 2E). The ratio of upper left to upper right quadrants was reversed (1:2) in thymocytes from *Atm*^{-/-} mice (Fig. 2F), indicating a significant increase in cells that exhibited a lower $\Delta\psi_m$. Addition of tempol to the thymocytes of all genotypes increased the number of cells with higher $\Delta\psi_m$ and enhanced the ratio of red/green fluorescence (Fig. 2G, H and M). In the case of thymocytes from the *Atm*^{-/-} mice, the $\Delta\psi_m$ was increased up to the range of untreated controls (compare Fig. 2E and H). To confirm that these effects were the result of oxidative stress, we used extracellular hypoxanthine (HX) and xanthine oxidase (XOD) to subject the cells to ROS. XOD converts HX to uric acid and as a by-product the enzyme generates H₂O₂ and superoxide radicals (O_2^-). This treatment greatly lowered the $\Delta\psi_m$ in the wild-type and *Atm*^{-/-} thymocytes (Fig. 2I and J). Again, tempol supplementation significantly increased the $\Delta\psi_m$ in thymocyte populations of the *Atm*^{-/-} thymocytes (Fig. 2K, L and M). The results provide further evidence that thymocytes from the *Atm*^{-/-} mice display higher levels of ROS and lower $\Delta\psi_m$ than the wild-type mice. In addition, tempol reduced ROS and restored higher, more normal $\Delta\psi_m$.

To test whether tempol could not only reduce but also protect cells from ROS, the wild-type and *Atm*^{-/-} thymocytes were treated with HX/XOD, in the presence or absence of tempol, and cell viability was measured using an MTT [3-(4,5 dimethylthiazol-2-yl)-2,5-diphenyl tetrazolium bromide] viability assay (44). After 18 h in culture, no toxic effects of tempol were observed in the wild-type and *Atm*^{-/-} thymocytes at concentrations up to 1 mM (data not shown). Tempol treatment (1 mM) resulted in significant protection to cells subjected to extracellular HX/XOD oxidative stress after 4 h of treatment, with little toxic effect in the absence of oxidative stress (Fig. 3A). It should be noted that previous studies (45,46) suggested that high concentrations

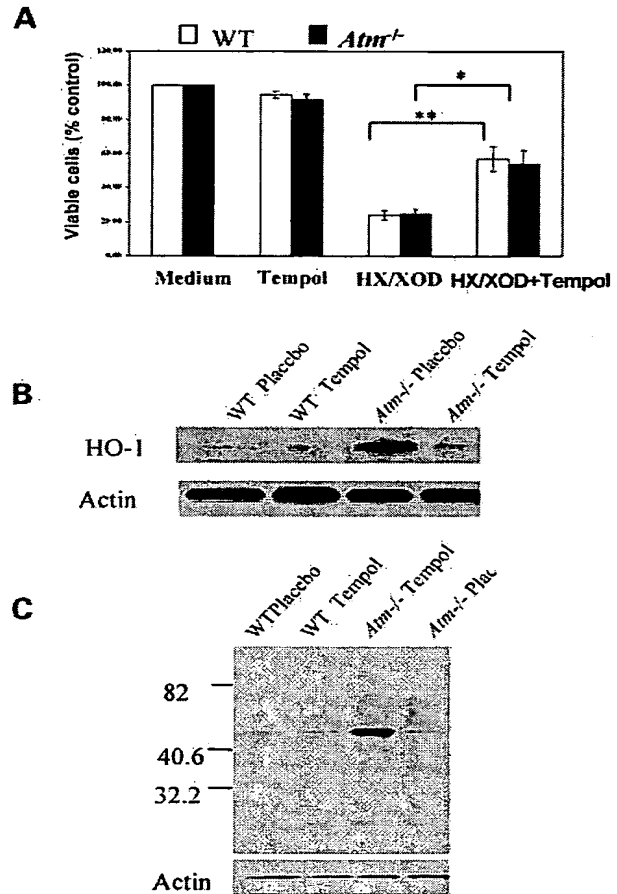


Figure 3. Oxidative damage and stress after tempol treatment *in vitro* and *in vivo*. (A) MTT survival analysis of primary thymocytes from the wild-type (white) and *Atm*^{-/-} (black) mice that were untreated (medium), treated with tempol (tempol), treated with an extracellular oxidative insult (HX/XOD) and treated with an oxidative insult plus tempol (HX/XOD + tempol). Levels of oxidative stress and oxidative damage in the thymus of control and tempol-treated mice were measured by western blot analysis of HO-1 levels (B) and oxidized protein carbonyl groups (C), respectively (**P* < 0.05; ***P* < 0.01).

of tempol could decrease the number of tumor cells in S and G2/M phase due to apoptosis. However, we did not observe apoptotic or necrotic cell death at concentrations up to 1 mM, suggesting that tempol treatment did not induce cell death.

Markers of oxidative stress such as heme-oxygenase-1 (HO-1) are increased in brain tissue of the *Atm*-deficient mice (19). As expected for an antioxidant, tempol treatment reduced HO-1 levels in the brain as measured by immunohistochemistry (data not shown). To determine if this marker of oxidative stress was also reduced in the thymus after tempol treatment, we performed western blot analysis to determine the levels of HO-1 protein in the thymus (the tissue where thymic lymphomas arise). Consistent with the brain, HO-1 was elevated in thymus from the *Atm*-deficient mice compared with the wild-type thymus (Fig. 3B) and tempol treatment

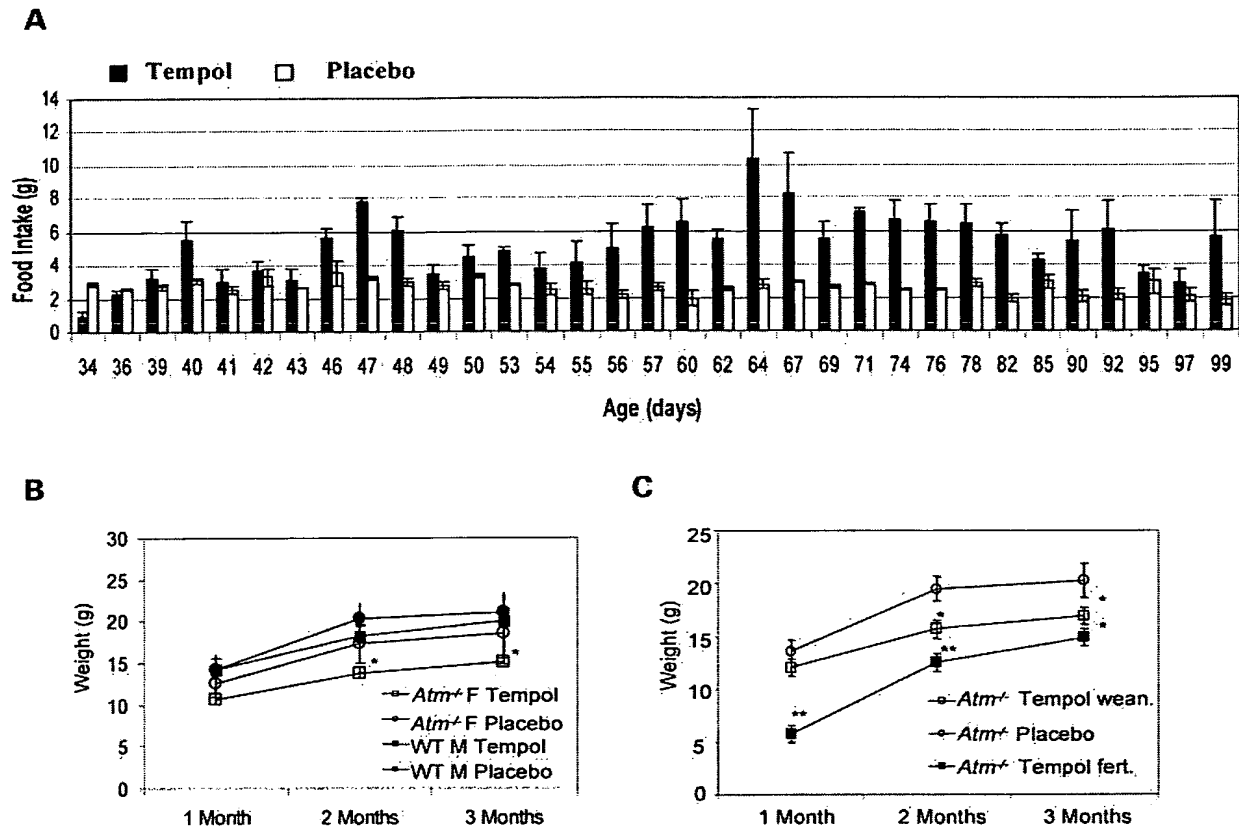


Figure 4. Effect of tempol treatment on food intake and weight gain of the *Atm*^{-/-} and wild-type mice. (A) Food consumption of the *Atm*^{-/-} mice treated with tempol or placebo at weaning. (B) Weight data of the *Atm*^{-/-} and wild-type mice treated with tempol or placebo at weaning. *Atm*^{-/-} tempol treated mice. (C) Weight data of *Atm*^{-/-} mice treated with tempol or placebo at weaning and from fertilization. Weights were taken at 1, 2, and 3 of age. For (B) and (C), significant values compare *Atm*^{-/-} mice fed placebo with *Atm*^{-/-} mice fed tempol (* $P < 0.05$; ** $P < 0.01$).

lowered these elevated levels of HO-1 in the thymus (Fig. 3B). To investigate whether tempol decreased oxidative damage, we measured protein damage as carbonyl derivatives on oxidized proteins via western blot analysis (Oxyblot) (47). The *Atm*-deficient thymus displayed markedly increased levels of oxidized proteins, whereas tempol treatment lowered the levels of oxidative damage to proteins in the thymocytes of treated *Atm*^{-/-} mice (Fig. 3C). Taken together, these data demonstrate that the chemopreventative effects of tempol are associated with broad antioxidant effects, including reduced ROS, oxidative stress and oxidative damage.

Tempol treatment resulted in lowered weight gain of the *Atm*^{-/-} mice

Although we used bacon-flavored chow in our study, we wanted to confirm that decreased food intake was not responsible for the observed chemopreventative effect of tempol, since caloric restriction has been shown to increase lifespan in both the wild-type, *p53*^{-/-} mice and other tumor prone mice (48–51). Tempol-treated *Atm*^{-/-} mice did not show a decrease in food intake compared with placebo (Fig. 4A), arguing against a role for caloric restriction in the

chemopreventative effect. However, tempol treatment for 1 month caused significant reduction in weight gain in the *Atm*^{-/-} mice (2 months old) treated at weaning (Fig. 4B and C), but no differences were found in the wild-type mice treated with tempol (Fig. 4B). The *Atm*^{-/-} mice treated from fertilization display significant reduction of weight from weaning (1 month) and maintained this difference over 3 months (Fig. 4C), although there was no effect on survival in this group of mice (Fig. 1B).

Tempol does not decrease metabolic rate or physical activity

To further investigate the weight reduction phenotype of the tempol-treated mice, we determined whether tempol treatment resulted in alterations in metabolism or activity. The tempol- and placebo-treated mice were studied in Comprehensive Lab Animal Monitoring Systems (CLAMS, Columbus Instruments). CLAMS are automated metabolic cages that allow non-invasive data collection of oxygen consumption, carbon dioxide production, physical activity, as well as food and water consumption. The wild-type mice were first studied in order to eliminate any confounding effects of genotype. Although the

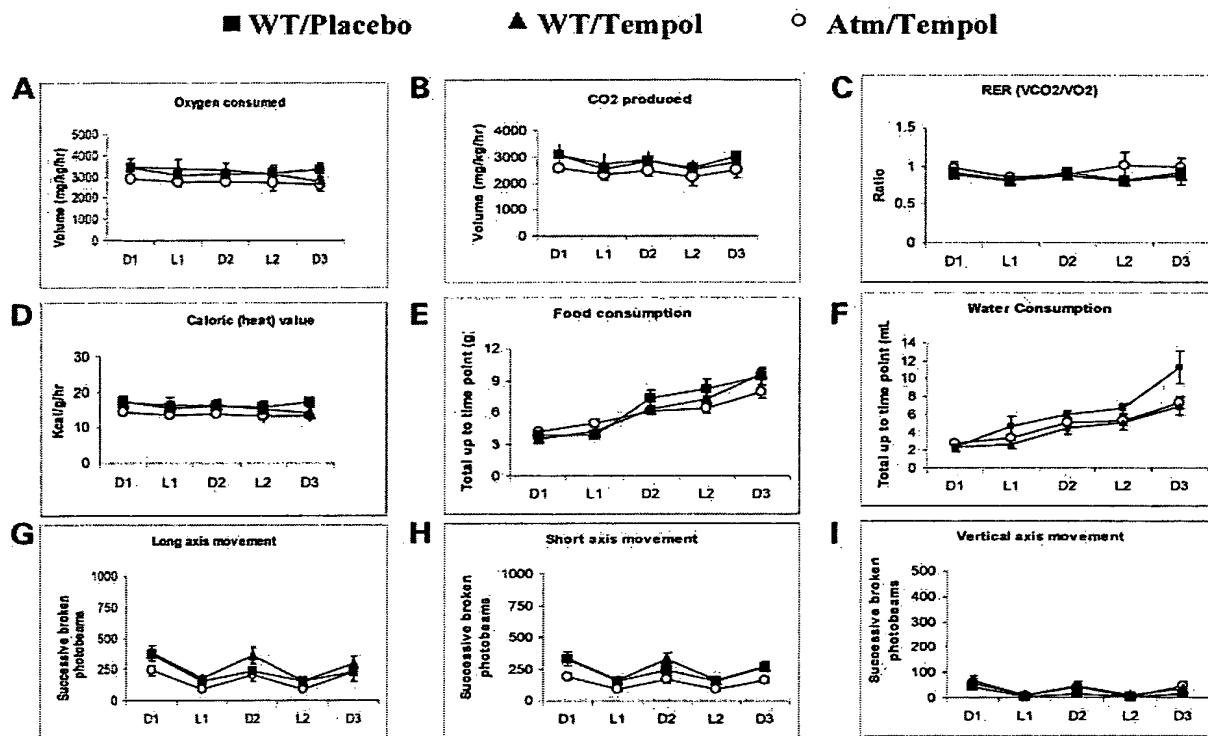


Figure 5. Metabolic rate and physical activity levels of the tempol- and placebo-treated wild-type mice, and the *Atm*^{-/-} tempol-treated mice. Metabolic parameters were measured over 3 days using CLAMS metabolic cages (Columbus Instruments) for the wild-type mice treated with (closed triangles, *n* = 7) and without tempol (closed circles, *n* = 6), and *Atm*^{-/-} tempol-treated mice (open circles, *n* = 6). X-axis displays two light cycles (L1–L2) and three dark cycles (D1–D3). (A) Total oxygen consumed; (B) CO₂ production; (C) respiration index (RER); (D) caloric (heat) production; (E) food consumption; (F) water consumption; (G) long axis movement; (H) short axis movement and (I) vertical axis movement (rearing).

wild-type placebo mice drank more water (Fig. 5F), no difference was observed in O₂ consumption (Fig. 5A), CO₂ production (Fig. 5B), respiration rate (RER) (Fig. 5C), caloric heat output (Fig. 5D), food consumption (Fig. 5E), or activity (Fig. 5G–I) between the tempol-treated and placebo mice. Our previous observation that food consumption was not decreased in the tempol chow group was replicated using the CLAMS cages. Metabolic rates were not significantly different between the tempol and placebo mice. In addition, the level of activity and the diurnal cycles of the mice were not affected by tempol treatment (Fig. 5G–I). Further, when water and food consumptions are corrected for mouse weight, there was no difference between the tempol-treated and placebo mice (data not shown). Similar results were found with the *Atm*-deficient mice treated with tempol (Fig. 5, *n* = 6), but due to technical difficulties with the CLAMS apparatus the *Atm*^{-/-} placebo fed mice could not be studied.

Tempol reduced proliferation of thymocytes and splenocytes

As noted above, ROS appear to have necessary signaling functions in the modulation of proliferative signaling pathways (3–8). The weight reducing effect of tempol on the *Atm*-

deficient mice suggests that proliferation might be affected by tempol treatment. In support of this interpretation, tempol treatment showed a trend in reduced cell number in the thymus (Fig. 6A) and other organs (data not shown) of the *Atm*^{-/-} as well as wild-type mice. To directly test whether tempol treatment resulted in anti-proliferative effects, we cultured splenocytes in the presence of phorbol 12-myristate 13-acetate (PMA) with and without 0.1 mM tempol. Tempol treatment had no effect on resting splenocytes but it significantly reduced proliferation in the PMA-induced *Atm*^{-/-} and wild-type cells (Fig. 6B).

DISCUSSION

Although there have been tremendous advances in understanding the genetic basis of tumorigenesis in multiple systems, cancer is still the second leading cause of death in the United States and most industrialized countries. It is estimated that 500 000 Americans die of cancer each year (52). Even with molecular advances that have identified genetic lesions that cause cancer, we still rely upon chemotherapy and radiation treatment to treat cancer patients. Such treatments are given to seriously ill patients and result in serious, sometimes fatal, side-effects. The development of genetic tests to determine an individual's susceptibility to cancer will

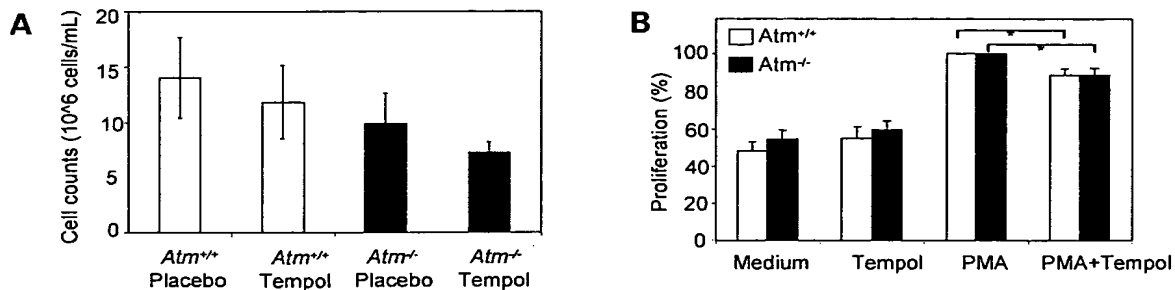


Figure 6. Tempol reduced proliferation of thymocytes and splenocytes. (A) Cell counts of thymocytes from the *Atm*^{-/-} and wild-type mice treated with tempol and placebo at weaning. (B) Percentage of cellular proliferation measured by MTT assay. Splenocytes from *Atm*^{-/-} and wild-type mice stimulated with PMA (1 ng/ml) and ionomycin (0.5 µg/ml) with and without tempol (0.1 mM). Values are shown as mean ± SEM (**P* < 0.05).

underscore the importance of devising strategies for cancer prevention, and to test these strategies in suitable animal models.

There is a growing interest in the chemopreventative ability of antioxidants in many naturally occurring products, from vitamin E to grape skin extract (resveratrol) (53). In some cases these agents have been shown to lower ROS and oxidative damage, inhibit cellular proliferation or induce apoptosis in transformed cells (54). ROS are attractive endogenous agents that are known to cause DNA mutagenesis and are intimately linked with cellular transformation. In addition, the signaling function of ROS in the modulation of apoptotic, stress and proliferative signaling pathways (3–8) further suggest that ROS may be an important target for cancer chemoprevention.

Here, we tested this hypothesis in a mouse model of the human tumor prone syndrome AT. In addition to the high cancer incidence, patients with AT as well as the *Atm*-deficient mice display increased oxidative stress and damage (19,55), and it has been proposed that this contributes to the tumor phenotype. Thus, *Atm*-deficient mice provide an excellent model to investigate the effect of antioxidants on tumorigenesis.

Long-term administration of the nitroxide tempol via the diet after weaning increased the latency to thymic lymphomas in the *Atm*-deficient mice (Fig. 1), without a change in the tumor type characteristic of this tumor prone model. As expected for an effective antioxidant, tempol treatment reduced ROS, restored mitochondrial membrane potential and reduced tissue oxidative damage and oxidative stress in the *Atm* mutant mice, both *in vitro* and *in vivo* (Figs 2 and 3). In this regard, our results are consistent with the notion that the chemopreventative effects of tempol are due to its antioxidant properties (36). Supporting this hypothesis, a recent study demonstrated that the antioxidant EUK-189 reversed the neurobehavioral deficit of *Atm*-deficient mice (56). *Atm*-deficient mice treated with EUK-189 also lived longer than untreated controls, presumably from a prolonged latency to tumorigenesis. EUK-189 is a salen-manganese compound that, like tempol, has catalase and superoxide dismutase activities (57). Thus, two distinct chemical types of antioxidants that have similar synthetic catalytic activities act to prolong the lifespan of *Atm*-deficient mice.

Many types of cancer cells have elevated ROS, and cellular proliferation can be inhibited by antioxidants, pointing to a critical role of ROS in cell growth (58). Tempol treatment resulted in reduced thymus size (data not shown) and cell number (Fig. 6A), and tempol reduced the proliferative capacity of splenocytes in culture (Fig. 6B). The anti-proliferative effect of tempol on PMA stimulated cells, but not on resting cells (Fig. 6B), suggests that this is a key effect of tempol and indicates a more general role of this nitroxide in proliferative signaling pathways. Thus, tempol's chemopreventative effect may be mediated through a reduction in cellular proliferation. A role for ROS and oxidative stress has been proposed for stimulation of cell proliferation as well as for cell depletion by apoptosis (59,60). In this regard, the antiproliferative effect of tempol might be due to its anti-oxidant properties. A reduction in tumor growth may increase lifespan of these mice by slowing down the time for the tumor burden to be great enough to compromise viability. Furthermore, there was also a significant reduction in weight in the *Atm* mutant mice fed tempol (Fig. 4B). This weight reduction was not a result of decreased food intake (Fig. 4A), lowered metabolism (Fig. 5) or physical inactivity (Fig. 5). Taken together, these data support the hypothesis that the chemopreventative effects of tempol may be due to a reduction in cellular proliferation. Further experiments will be needed to test this hypothesis in more detail.

Because ROS have also been implicated in cellular senescence and apoptosis (58) it is also formally possible that tempol may cause changes in apoptosis, either in the general cell population or specifically in the transformed cells. This could account for the decrease in proliferation and the reduced body size, organ size and thymus cellularity in the tempol fed mice. However, we found no evidence that tempol acts as an inducer of programmed cell death, as shown by the MTT assay (Fig. 3A), as well as the restoration of mitochondrial membrane potential in the *Atm*-deficient mice to the wild-type levels (Fig. 2B). The mitochondrial membrane is a target of ROS, and decreasing potential is an early marker of apoptosis (42). We found that the effect of tempol was to increase mitochondrial membrane potential. Also, a change in apoptosis in the thymus should result in changes in thymocyte maturation, reflected by the number of CD4⁺ and CD8⁺

single positive and double positive thymocytes. We have seen no change in these thymocyte populations *in vivo* with tempol treatment (data not shown). Finally, tempol does not have an acute apoptotic effect on transformed cells, since thymoma cell lines treated with tempol for up to 18 h show no change in survival (data not shown). Thus, our data does not support the hypothesis that tempol causes changes in apoptosis.

The data also argue against the possibility that the chemopreventative effect of tempol was due to caloric restriction. Caloric restriction has been shown to reduce oxidative stress and ROS as well as to increase the lifespan of *p53*^{-/-} mice (48–51). First, there was no decrease in bacon-flavored tempol food intake in both the *Atm*^{-/-} and wild-type mice when compared with the placebo. Food intake was also the same in the C3H mice fed bacon-flavored chow with (tempol) or without (placebo) tempol (36). Second, while caloric restriction has been shown to change tumor spectrum (48–51) tempol treatment did not have any effect on tumor type in the *Atm*^{-/-} or C3H mice (36). Third, there was no effect on latency to tumors in the *Atm*^{-/-} mice treated with tempol from fertilization although these mice were much smaller than the wild-type or *Atm*^{-/-} mice that were treated with tempol at weaning. This group displayed more severe side-effects in general, such as embryonic and perinatal lethality and hyperactivity. The lack of tempol chemoprevention in this group may be due to compensating mechanisms to tempol treatment that allows some of the mice to survive. The adverse effects seen in this treatment group were not noted in mice treated with tempol at weaning, nor were they noted in a large cohort of the C3H mice treated after weaning throughout their lifetime with similar tempol doses (36).

In summary, our findings demonstrate that tempol has significant chemopreventative effects on a cancer prone mouse model. Because the *Atm*-deficient mice are a good model of many aspects of human AT, our results raise the possibility that tempol could be used in the chemoprevention of tumors in humans with cancer prone syndromes, and may be especially effective in those associated with oxidative stress.

MATERIALS AND METHODS

Mice and tempol treatment

Atm-deficient mice (37), in 129SvEv background, were used and all animal procedures were performed according to protocols approved by both the NIH ACUC and the UCSD Animal Subjects Committee. Powdered tempol was purchased from Aldrich (Milwaukee, WI, USA) and was mixed with bacon-flavored mouse chow (Bio-Serv, NJ, USA) at a concentration equivalent to 58 mM (10 mg/g of food). Sixty-seven *Atm*^{-/-} mice (32 males and 35 females) were separated into three groups: 40 mice (22 males and 18 females) received bacon-flavored placebo chow; 17 mice (five males and 12 females) were treated with tempol started in the females prior to mating; 10 mice (five males and five females) were treated with tempol starting at weaning (3 weeks old). Mice were checked weekly for tumors, and sacrificed when thymic lymphomas were detectable. The presence of tumors was

confirmed histologically, and karyotype analysis was performed to determine the presence of translocations or aneuploidy.

Weight and food intake

The cohort of mice used in the survival study (mentioned earlier) and new cohort were combined for the weight data. Eighteen *Atm*^{-/-} placebo (10 males, eight females) and 20 *Atm*^{-/-} tempol (six males, 14 females) treated mice. Weight was taken at 1, 2 and 3 months of age. Food intake was measured every other day by weighing the difference between food placed in the cage and what was left for 10 *Atm*^{-/-} mice treated with tempol (*n* = 5) and with placebo (*n* = 5). Food intake was measured for the 3 months between the ages of 34 and 99 days. Mice that did not survive the duration of the food intake study were not included.

Metabolic measurements

Six pairs of age matched wild-type mice from the tempol and placebo food groups were placed in CLAMS metabolic cages (Columbus Instruments, Columbus, OH, USA). These metabolic chambers monitor activity, food and water consumptions, and metabolic performance. Data were collected every 30 min over three 12 h dark cycles and two 12 h light cycles. The metabolic measurements included the volume of carbon dioxide produced (VCO_2), the volume of oxygen consumed (VO_2), the respiration measurement ($RER = VCO_2/VO_2$) and the caloric (heat) value: $\{[(3.815 + 1.232 \times RER) \times VO_2] \times 1000\}$ /mouse weight. The data are represented as the mean values over each 12 h period.

Measuring intracellular ROS in thymocytes

Thymi were isolated from the 1-month-old *Atm*^{+/+} and *Atm*^{-/-} mice. Tempol was dissolved in phosphate buffered saline (PBS). Cells were untreated or treated with 10 μ M tempol for 30 min, collected and resuspended in 1 ml PBS containing 10 μ M DCF diacetate (Molecular Probes, Inc., OR, USA) for 30 min. Cells were labeled with PE- α CD4 and APC- α CD8a (BD PharMingen, CA, USA), stained with 7AAD, and analyzed by flow cytometry on a Coulter Epics Elite (Beckman Coulter, Inc., CA, USA). The FITC signals from DCF in live cells were determined for CD4/CD8 double positive cells, since this is the population from which tumors arise (37,38). Six independent experiments were performed.

Mitochondrial membrane potential ($\Delta\psi_m$)

Control thymocytes and cells treated for 4 h with 0.1 mM HX and 10 mU XOD with and without 1 mM tempol were incubated for 15 min at 37°C with 10 μ g/ml JC-1 (Molecular Probes, Eugene, OR, USA), washed twice with PBS, resuspended in a total volume of 400 μ l PBS, and 10 000 cells per sample were analyzed by flow cytometry (43). Data analysis was performed with Coulter Epics Elite software version 4.1 (Beckman Coulter Inc., Fullerton, CA, USA).

MTT assay

Mitochondrial respiration and cellular activity was measured in thymocytes via the MTT assay (44). For proliferation studies, splenocytes were treated with PMA (1 ng/ml) and ionomycin (0.5 µg/ml) for 24 h. For survival, thymocytes were treated with 0.1 mM HX (Sigma, St Louis, MO, USA), 10 mU XOD (Boehringer Mannheim, Germany) for 4 and 18 h with and without 0.1 mM and 1 mM tempol, respectively. PBS with 0.5 mg/ml MTT (Sigma) was added and the cells were incubated further for 4 h at 37°C. The blue-colored water-insoluble product that is converted from the yellow MTT by the cells was dissolved in 0.04 M HCl in isopropanol for 5 min and colorimetrically quantified (absorbance 570 nm, reference 630 nm).

Western blot analysis

Thymi of age-matched mice (average of 17 months of age), fed tempol or placebo food, were used for analysis of HO-1 protein expression by western blot analysis as previously described (61). Protein was electrophoresed on a 4–20% Tris–glycine gel (Invitrogen, CA, USA), and transferred to polyvinylidene difluoride membranes (Millipore, MA, USA). Primary antibodies HO-1 (Stressgen SPA-895) and actin (Santa Cruz Biotech, Santa Cruz, CA, USA, sc-1616) were incubated at 1:500 in 3% milk TBS-T overnight at 4°C. Following incubation with peroxidase-conjugated secondary antibodies (1:5000), the proteins were visualized by chemiluminescence detection system (Pierce Super Signal West Pico, Pierce, IL, USA). To detect the level of oxidized proteins, we used the Intergen Oxyblot kit (according to the manufacturer's protocol) to assess the level of oxidized protein carbonyl groups. Protein samples were prepared from age matched mice fed placebo or tempol-treated food as stated above. A non-derivatized negative control was run to ensure that non-specific bands were not being detected.

Statistical analysis

Survival time of mice was used to generate Kaplan–Meier survival curves that were compared using log-rank (Mantel–Cox) test. A Cox proportional-hazard regression analysis was used to adjust for the potential effect of gender. A two factorial analysis of variance (genotype × treatment) were used to analyze data from measuring intracellular ROS in thymocytes and the comet assay. *Post hoc* comparisons were made using Scheffe's *F* and Fisher's protected least significant difference test for measuring intracellular ROS in thymocytes. For the MTT assays and mitochondrial membrane potential (JC-1) an unpaired Student's *t*-test was performed.

ACKNOWLEDGEMENTS

We would like to thank Judy Nordberg at the San Diego VA Hospital FACS Core for help and advice with flow cytometry, Jeff Long for assistance with the CLAMS experiments, Amy Sullivan, Jennifer MacArthur and Scott E. Williams for technical help, and Web Cavenee, Geoff Rosenfeld, Steve Dowdy and Yutaka Sagara for advice and comments on the

manuscript. This work was supported by intramural funds from the NHGRI, institutional funds from UCSD School of Medicine and an institutional grant from HHMI. The authors declare that they have no competing financial interests.

REFERENCES

- Davies, K.J. (2000) Oxidative stress, antioxidant defenses, and damage removal, repair, and replacement systems. *IUBMB Life*, **50**, 279–289.
- Beckman, K.B. and Ames, B.N. (1997) Oxidative decay of DNA. *J. Biol. Chem.*, **272**, 19633–19636.
- Burdon, R.H. (1995) Superoxide and hydrogen peroxide in relation to mammalian cell proliferation. *Free Radic. Biol. Med.*, **18**, 775–794.
- Schmidt-Ullrich, R.K., Dent, P., Grant, S., Mikkelsen, R.B. and Valerie, K. (2000) Signal transduction and cellular radiation responses. *Radiat. Res.*, **153**, 245–257.
- Pearce, A.K. and Humphrey, T.C. (2001) Integrating stress-response and cell-cycle checkpoint pathways. *Trends Cell Biol.*, **11**, 426–433.
- Finkel, T. (2001) Reactive oxygen species and signal transduction. *IUBMB Life*, **52**, 3–6.
- Leroy, C., Mann, C. and Marsolier, M.C. (2001) Silent repair accounts for cell cycle specificity in the signaling of oxidative DNA lesions. *EMBO J.*, **20**, 2896–2906.
- Sauer, H., Wartenberg, M. and Hescheler, J. (2001) Reactive oxygen species as intracellular messengers during cell growth and differentiation. *Cell Physiol. Biochem.*, **11**, 173–186.
- Neumann, C.A., Krause, D.S., Carman, C., Das, S., Dubey, D., Abraham, J., Bronson, R.T., Fujiwara, Y., Orkin, S. and Van Etten, R. (2003) Essential role for the peroxiredoxin Prdx1 in erythrocyte antioxidant defence and tumour suppression. *Nature*, **424**, 561–565.
- Tamimi, R.M., Lagiou, P., Adami, H.O. and Trichopoulos, D. (2002) Prospects for chemoprevention of cancer. *J. Intern. Med.*, **251**, 286–300.
- Savitsky, K., Bar-Shira, A., Gilad, S., Rotman, G., Ziv, Y., Vanagaite, L., Tagle, D.A., Smith, S., Uziel, T., Sfez, S. *et al.* (1995) A single ataxia telangiectasia gene with a product similar to PI-3 kinase. *Science*, **268**, 1749–1753.
- Keith, C.T. and Schreiber, S.L. (1995) PIK-related kinases: DNA repair, recombination, and cell cycle checkpoints. *Science*, **270**, 50–51.
- Kastan, M.B. and Lim, D.S. (2000) The many substrates and functions of ATM. *Nat. Rev. Mol. Cell Biol.*, **1**, 179–186.
- Abraham, R.T. (2001) Cell cycle checkpoint signaling through the ATM and ATR kinases. *Genes Dev.*, **15**, 2177–2196.
- Shiloh, Y. (1997) Ataxia-telangiectasia and the Nijmegen breakage syndrome: related disorders but genes apart. *Annu. Rev. Genet.*, **31**, 635–662.
- Rotman, G. and Shiloh, Y. (1997) Ataxia-telangiectasia: is ATM a sensor of oxidative damage and stress? *Bioessays*, **19**, 911–917.
- Takao, N., Li, Y. and Yamamoto, K. (2000) Protective roles for ATM in cellular response to oxidative stress. *FEBS Lett.*, **472**, 133–136.
- Formichi, P., Battisti, C., Tripodi, S.A., Tosi, P. and Federico, A. (2000) Apoptotic response and cell cycle transition in ataxia telangiectasia cells exposed to oxidative stress. *Life Sci.*, **66**, 1893–1903.
- Barlow, C., Denner, P.A., Shigenaga, M.K., Smith, M.A., Morrow, J.D., Roberts, L.J., II, Wynshaw-Boris, A. and Levine, R.L. (1999) Loss of the ataxia-telangiectasia gene product causes oxidative damage in target organs. *Proc. Natl Acad. Sci. USA*, **96**, 9915–9919.
- Kamsler, A., Daily, D., Hochman, A., Stern, N., Shiloh, Y., Rotman, G. and Barzilai, A. (2001) Increased oxidative stress in ataxia telangiectasia evidenced by alterations in redox state of brains from Atm-deficient mice. *Cancer Res.*, **61**, 1849–1854.
- Quick, K.L. and Dugan, L.L. (2001) Superoxide stress identifies neurons at risk in a model of ataxia-telangiectasia. *Ann. Neurol.*, **49**, 627–635.
- Stern, N., Hochman, A., Zemach, N., Weizman, N., Hammel, I., Shiloh, Y., Rotman, G. and Barzilai, A. (2002) Accumulation of DNA damage and reduced levels of nicotinic adenine dinucleotide in the brains of Atm-deficient mice. *J. Biol. Chem.*, **277**, 602–608.
- Krishna, M.C., Grahame, D.A., Samuni, A., Mitchell, J.B. and Russo, A. (1992) Oxoammonium cation intermediate in the nitroxide-catalyzed dismutation of superoxide. *Proc. Natl Acad. Sci. USA*, **89**, 5537–5541.
- Samuni, A.M., DeGraff, W., Krishna, M.C. and Mitchell, J.B. (2002) Nitroxides as antioxidants: tempol protects against EO9 cytotoxicity. *Mol. Cell. Biochem.*, **234–235**, 327–333.

25. Thiernemann, C. (2003) Membrane-permeable radical scavengers (tempol) for shock, ischemia-reperfusion injury, and inflammation. *Crit. Care Med.*, **31**, S76–S84.
26. Thiernemann, C., McDonald, M.C. and Cuzzocrea, S. (2001) The stable nitroxide, tempol, attenuates the effects of peroxynitrite and oxygen-derived free radicals. *Crit. Care Med.*, **29**, 223–224.
27. Hahn, S.M., Tochner, Z., Krishna, C.M., Glass, J., Wilson, L., Samuni, A., Sprague, M., Venzon, D., Glatstein, E., Mitchell, J.B. *et al.* (1992) Tempol, a stable free radical, is a novel murine radiation protector. *Cancer Res.*, **52**, 1750–1753.
28. Weiss, L., Stern, S., Reich, S. and Slavin, S. (1993) Effect of recombinant human manganese superoxide dismutase on radiosensitivity of murine B cell leukemia (BCL1) cells. *Leuk. Lymphoma*, **10**, 477–481.
29. Samuni, A., Krishna, C.M., Riesz, P., Finkelstein, E. and Russo, A. (1988) A novel metal-free low molecular weight superoxide dismutase mimic. *J. Biol. Chem.*, **263**, 17921–17924.
30. Krishna, M.C., Samuni, A., Taira, J., Goldstein, S., Mitchell, J.B. and Russo, A. (1996) Stimulation by nitroxides of catalase-like activity of hemoproteins. Kinetics and mechanism. *J. Biol. Chem.*, **271**, 26018–26025.
31. Monti, E., Cova, D., Guido, E., Morelli, R. and Oliva, C. (1996) Protective effect of the nitroxide tempol against the cardiotoxicity of adriamycin. *Free Radic. Biol. Med.*, **21**, 463–470.
32. Reddan, J., Sevilla, M., Giblin, F., Padgaonkar, V., Dziedzic, D. and Leverenz, V. (1992) Tempol and deferoxamine protect cultured rabbit lens epithelial cells from H₂O₂ insult: insight into the mechanism of H₂O₂-induced injury. *Lens Eye Toxic. Res.*, **9**, 385–393.
33. Mitchell, J.B., Samuni, A., Krishna, M.C., DeGraff, W.G., Ahn, M.S., Samuni, U. and Russo, A. (1990) Biologically active metal-independent superoxide dismutase mimics. *Biochemistry*, **29**, 2802–2807.
34. Rak, R., Chao, D.L., Pluta, R.M., Mitchell, J.B., Oldfield, E.H. and Watson, J.C. (2000) Neuroprotection by the stable nitroxide tempol during reperfusion in a rat model of transient focal ischemia. *J. Neurosurg.*, **92**, 646–651.
35. Samuni, A., Winkelsberg, D., Pinson, A., Hahn, S.M., Mitchell, J.B. and Russo, A. (1991) Nitroxide stable radicals protect beating cardiomyocytes against oxidative damage. *J. Clin. Invest.*, **87**, 1526–1530.
36. Mitchell, J.B., Xavier, S., DeLuca, A.M., Sowers, A.L., Cook, J.A., Krishna, M.C., Hahn, S.M. and Russo, A. (2003) A low molecular weight antioxidant decreases weight and lowers tumor incidence. *Free Radic. Biol. Med.*, **34**, 93–102.
37. Barlow, C., Hirotsune, S., Paylor, R., Liyanage, M., Eckhaus, M., Collins, F., Shiloh, Y., Crawley, J.N., Ried, T., Tagle, D. *et al.* (1996) Atm-deficient mice: a paradigm of ataxia telangiectasia. *Cell*, **86**, 159–171.
38. Liyanage, M., Weaver, Z., Barlow, C., Coleman, A., Pankratz, D.G., Anderson, S., Wynshaw-Boris, A. and Ried, T. (2000) Abnormal rearrangement within the alpha/delta T-cell receptor locus in lymphomas from Atm-deficient mice. *Blood*, **96**, 1940–1946.
39. Burrow, S. and Valet, G. (1987) Flow-cytometric characterization of stimulation, free radical formation, peroxidase activity and phagocytosis of human granulocytes with 2,7-dichlorofluorescein (DCF). *Eur. J. Cell Biol.*, **43**, 128–133.
40. Watanabe, S. (1998) *In vivo* fluorometric measurement of cerebral oxidative stress using 2'-7'-dichlorofluorescein (DCF). *Keio J. Med.*, **47**, 92–98.
41. Wang, H. and Joseph, J.A. (1999) Quantifying cellular oxidative stress by dichlorofluorescein assay using microplate reader. *Free Radic. Biol. Med.*, **27**, 612–616.
42. Melov, S. (2002) Therapeutics against mitochondrial oxidative stress in animal models of aging. *Ann. NY Acad. Sci.*, **959**, 330–340.
43. Cossarizza, A., Baccarani-Contri, M., Kalashnikova, G. and Franceschi, C. (1993) A new method for the cytofluorimetric analysis of mitochondrial membrane potential using the J-aggregate forming lipophilic cation 5,5',6,6'-tetrachloro-1,1',3,3'-tetraethylbenzimidazolcarbocyanine iodide (JC-1). *Biochem. Biophys. Res. Commun.*, **197**, 40–45.
44. Mossmann (1983) Rapid colorimetric assay for cellular growth and survival: application to proliferation and cytotoxicity assays. *J. Immunol. Methods*, **65**, 55–63.
45. Gariboldi, M.B., Lucchi, S., Caserini, C., Supino, R., Oliva, C. and Monti, E. (1998) Antiproliferative effect of the piperidine nitroxide TEMPOL on neoplastic and nonneoplastic mammalian cell lines. *Free Radic. Biol. Med.*, **24**, 913–923.
46. Monti, E., Supino, R., Colleoni, M., Costa, B., Ravizza, R. and Gariboldi, M.B. (2001) Nitroxide TEMPOL impairs mitochondrial function and induces apoptosis in HL60 cells. *J. Cell. Biochem.*, **82**, 271–276.
47. Singhal, A.B., Wang, X., Sumii, T., Mori, T. and Lo, E.H. (2002) Effects of normobaric hyperoxia in a rat model of focal cerebral ischemia-reperfusion. *J. Cereb. Blood Flow Metab.*, **22**, 861–868.
48. Berrigan, D., Perkins, S.N., Haines, D.C. and Hursting, S.D. (2002) Adult-onset calorie restriction and fasting delay spontaneous tumorigenesis in p53-deficient mice. *Carcinogenesis*, **23**, 817–822.
49. Hursting, S.D., Perkins, S.N., Brown, C.C., Haines, D.C. and Phang, J.M. (1997) Calorie restriction induces a p53-independent delay of spontaneous carcinogenesis in p53-deficient and wild-type mice. *Cancer Res.*, **57**, 2843–2846.
50. Pugh, T.D., Oberley, T.D. and Weindruch, R. (1999) Dietary intervention at middle age: caloric restriction but not dehydroepiandrosterone sulfate increases lifespan and lifetime cancer incidence in mice. *Cancer Res.*, **59**, 1642–1648.
51. Yoshida, K., Inoue, T., Nojima, K., Hirabayashi, Y. and Sado, T. (1997) Calorie restriction reduces the incidence of myeloid leukemia induced by a single whole-body radiation in C3H/He mice. *Proc. Natl Acad. Sci. USA*, **94**, 2615–2619.
52. Edwards, B.K., Howe, H.L., Ries, L.A., Thun, M.J., Rosenberg, H.M., Yancik, R., Wingo, P.A., Jemal, A. and Feigal, E.G. (2002) Annual report to the nation on the status of cancer, 1973–1999, featuring implications of age and aging on U.S. cancer burden. *Cancer*, **94**, 2766–2792.
53. Krishnan, K., Campbell, S., Abdel-Rahman, F., Whaley, S. and Stone, W.L. (2003) Cancer chemoprevention drug targets. *Curr. Drug Targets*, **4**, 45–54.
54. Schwartz, J.L., Antoniadis, D.Z. and Zhao, S. (1993) Molecular and biochemical reprogramming of oncogenesis through the activity of prooxidants and antioxidants. *Ann. NY Acad. Sci.*, **686**, 262–278.
55. Reichenbach, J., Schubert, R., Schwan, C., Muller, K., Bohles, H.J. and Zielen, S. (1999) Anti-oxidative capacity in patients with ataxia telangiectasia. *Clin. Exp. Immunol.*, **117**, 535–539.
56. Browne, S.E., Roberts, L.J., 2nd, Dennery, P.A., Doctrow, S.R., Beal, M.F., Barlow, C. and Levine, R.L. (2004) Treatment with a catalytic antioxidant corrects the neurobehavioral defect in ataxia-telangiectasia mice. *Free Radic. Biol. Med.*, **36**, 938–942.
57. Doctrow, S.R., Huffman, K., Marcus, C.B., Tocco, G., Malfroy, E., Adinolfi, C.A., Kruk, H., Baker, K., Lazarowich, N., Mascarenhas, J. *et al.* (2002) Salen-manganese complexes as catalytic scavengers of hydrogen peroxide and cytoprotective agents: structure-activity relationship studies. *J. Med. Chem.*, **45**, 4549–4558.
58. Behrend, L., Henderson, G. and Zwacka, R.M. (2003) Reactive oxygen species in oncogenic transformation. *Biochem. Soc. Trans.*, **31**, 1441–1444.
59. Burdon, R.H. (1995) Superoxide and hydrogen peroxide in relation to mammalian cell proliferation. *Free Radic. Biol. Med.*, **18**, 775–794.
60. Slater, A.F., Stefan, C., Nobel, I., van den Dobbelen, D.J. and Orrenius, S. (1995) Signalling mechanisms and oxidative stress in apoptosis. *Toxicol. Lett.*, **82–83**, 149–153.
61. Sambrook, J., Fritsch, E.F. and Maniatis, T. (1989) *Molecular cloning: A Laboratory Manual*, 2nd edn. Cold Spring Harbor Laboratory Press.

**This Page is Inserted by IFW Indexing and Scanning
Operations and is not part of the Official Record**

BEST AVAILABLE IMAGES

Defective images within this document are accurate representations of the original documents submitted by the applicant.

Defects in the images include but are not limited to the items checked:

- ☐ BLACK BORDERS
- ☐ IMAGE CUT OFF AT TOP, BOTTOM OR SIDES
- ☐ FADED TEXT OR DRAWING
- ☒ BLURRED OR ILLEGIBLE TEXT OR DRAWING
- ☐ SKEWED/SLANTED IMAGES
- ☐ COLOR OR BLACK AND WHITE PHOTOGRAPHS
- ☐ GRAY SCALE DOCUMENTS
- ☐ LINES OR MARKS ON ORIGINAL DOCUMENT
- ☐ REFERENCE(S) OR EXHIBIT(S) SUBMITTED ARE POOR QUALITY
- ☐ OTHER: _____

IMAGES ARE BEST AVAILABLE COPY.

As rescanning these documents will not correct the image problems checked, please do not report these problems to the IFW Image Problem Mailbox.